



Performance of the MeV gamma-ray telescopes and polarimeters of the future

$\gamma \rightarrow e^+e^-$ in silicon-detector active targets

D. Bernard

LLR, Ecole Polytechnique, CNRS/IN2P3, 91128 Palaiseau, France
e-mail: denis.bernard@in2p3.fr

Abstract. A number of techniques are being developed to solve the monstrous sensitivity gap that exists between the energy ranges of good sensitivity of the Compton and of the pair telescopes and to extend polarimetry to the MeV gamma-ray world. I characterize the properties of an active target, detailing the various contributions to the angular resolution, using a full five-dimensional event generator of the Bethe-Heitler differential cross section. With the same tool I also examine the dilution of the polarization asymmetry induced by multiple scattering in the conversion wafer.

Key words. gamma-ray telescope – gamma-ray polarimeter – pair conversion – silicon detector – multiple scattering – event generator

1. Introduction

Facing the huge sensitivity gap between the energy ranges of the Compton and of the pair-creation telescopes (Fig. 1 of Schönfelder 2004), and given the absence of polarimetry measurements of cosmic sources with pair conversion, i.e. in the MeV energy range, a number of techniques are put forward to design high-performance MeV γ -ray telescopes and polarimeters: (1) gas detectors (HARPO Gros et al. 2018; Bernard 2018b); (2) emulsion detectors (GRAINE Takahashi et al. 2015; Ozaki et al. 2016); (3) silicon detectors (e-ASTROGAM De Angelis et al. 2018 and AMEGO Moiseev et al. 2018). These telescopes are based on the use of active targets, that is, a scheme in which the photon converts and the two leptons (the e^+ and the e^-) are tracked in the same detector.

I focus here on silicon detectors, providing simple analytical expressions that describe the various contributions to the angular resolution and examining the dilution of the polarization asymmetry due to multiple scattering in the conversion wafer.

2. Angular resolution

Upon the pair-conversion of an MeV γ ray in the field of a nucleus, the final state consists of three particles, the e^+e^- pair and the “recoiling” nucleus, to which a small (keV/ c to MeV/ c) momentum is transferred; the recoiling nucleus is therefore slow and its track length is too short to allow a measurement. The missing recoil momentum, q , contributes to the angular resolution. As the q -spectrum shows a tail to high values (Fig. 3 of Bernard 2013b), “containment values” at a given fraction are

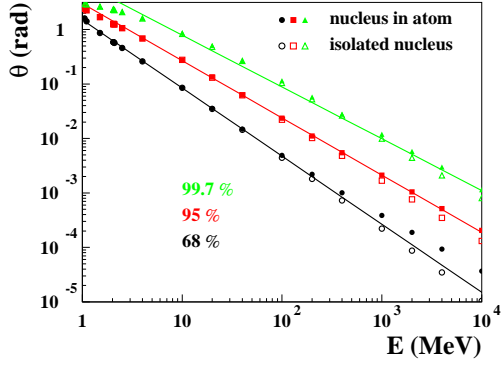


Fig. 1. Variation of the 68%, 95% and 99.7% containment values of the angular resolution due to the missing nucleus-recoil momentum, as a function of incident photon energy E (adapted from Gros & Bernard 2017a).

computed (Gros & Bernard 2017a and Fig. 1). The $1\text{-}\sigma$, $2\text{-}\sigma$ and $3\text{-}\sigma$ containment values are found to vary with the photon energy, E , approximately like

$$\begin{aligned} - \theta_{68\%} &\approx 1.5 \text{ rad } (E/\text{MeV})^{-1.25}, \\ - \theta_{95\%} &\approx 3.0 \text{ rad } (E/\text{MeV})^{-1.05}, \\ - \theta_{99.7\%} &\approx 7.0 \text{ rad } (E/\text{MeV})^{-0.95}. \end{aligned}$$

These results were obtained using an exact sampling of the five-dimensional Bethe-Heitler differential cross section (Bernard 2013a) that I have made available as the G4BetheHeitler5DModel physics model of the recently deployed 10.5 Geant4 release (Bernard 2018a). None of the pre-existing physics models were found to be appropriate for the simulation of the high-performance detectors that are being planned nor for polarization (Gros & Bernard 2017b).

MeV γ -ray conversions produce leptons with MeV/ c momentum that undergo significant multiple scattering in each wafer with an RMS deflection angle $\theta_0 \approx (p_0/p) \sqrt{e/X_0}$, where p is the track momentum, $p_0 = 13.6 \text{ MeV}/c$ is the multiple scattering constant (Tanabashi et al. 2018), e is the wafer thickness through which the lepton propagates and X_0 is the wafer material radiation length. Fitting the tracks with a Kalman filter allows multiple scattering to be taken into account together with the single-wafer spatial resolution in an optimal way, assuming Gaussian statistics. The

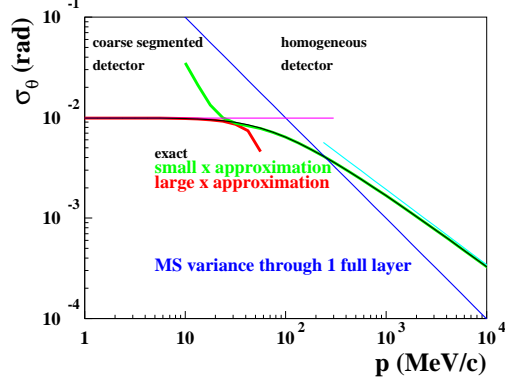


Fig. 2. Single-track angular resolution of a segmented detector as a function of track momentum (black curve). The small- x approximation, valid at high energies, is eq. (22) of Frosini & Bernard 2017, green curve (the cyan line is $\sigma_\theta \approx (p/p_1)^{-3/4}$). The high- x approximation, valid at low energies, is eq. (25) of Frosini & Bernard 2017, red curve (the magenta line is $\sigma_\theta \approx \sqrt{2}\sigma/l$).

(RMS) angular resolution of a segmented detector, σ_θ , is ¹ (Frosini & Bernard 2017)

$$\sigma_\theta = \frac{\sigma}{l} \sqrt{\frac{2x^3 (\sqrt{4j-x^2} + \sqrt{-4j-x^2})}{(\sqrt{4j-x^2} + jx)(\sqrt{-4j-x^2} - jx)}}, \quad (1)$$

where x is the distance between wafers, l , normalized to the detector scattering length λ (defined in eq. (17) of Frosini & Bernard 2017, see also Innes 1993), $x \equiv l/\lambda = \sqrt{(l/\sigma)(p_0/p) \sqrt{e/X_0}}$, σ is the precision of the measurement of the track position in a wafer, and j is the imaginary unit. The variation of σ_θ with p (Fig. 2) shows two regimes:

- at low momentum (large x), the coarsely-segmented detector approximation can be used, with $\sigma_\theta \approx \sqrt{2}\sigma/l$ (see eq. (25) of Frosini & Bernard 2017). An optimal measurement can be obtained simply from the position measurements in the two first wafers, no Kalman filter is needed.
- at high momentum (small x), the homogeneous detector approximation can be used,

¹ I have corrected a misprint.

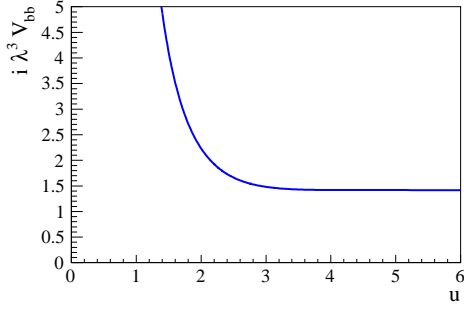


Fig. 3. Normalized angle variance as a function of the total detector thickness normalized to the detector scattering length, $u \equiv Nx = Nl/\lambda$, in the fully homogeneous detector approximation, $x = 0$ (several values of x were examined in Fig. 4 of Frosini & Bernard 2017).

$\sigma_\theta \approx (p/p_1)^{-3/4}$ where p_1 is a momentum that characterizes the tracking-with-multiple-scattering properties of the detector, $p_1 = p_0 (4\sigma^2 l^4 / X_0^3 e^3)^{1/6}$ (Bernard 2013a) see also eq. (22) of (see also eq. (22) of Frosini & Bernard 2017).

I used e-ASTROGAM numerical values of the detector parameters (De Angelis et al. 2018). These results were obtained assuming that the photon converted in the lowest part of a wafer. In the more general case of a conversion well within the wafer, the additional contribution of multiple scattering in the conversion wafer must be added (for the full thickness e , the blue line in Fig. 2).

The above results were obtained assuming that the detector is thick enough that the Kalman filter converged to an equilibrium: only the first part of the track contributes significantly to the angle measurement, after which multiple scattering floods it all. A detector is found to be thick for a thickness of at least 2.5 scattering lengths (Fig. 3, and Fig. 4 of Frosini & Bernard 2017), that is for $p < 72 \text{ GeV}/c$ for e-ASTROGAM. For most of the available momentum range, the optimum number of wafers is then quite small (Fig. 4). Fitting a longer track segment would expose the Kalman filter to un-necessary bias induced

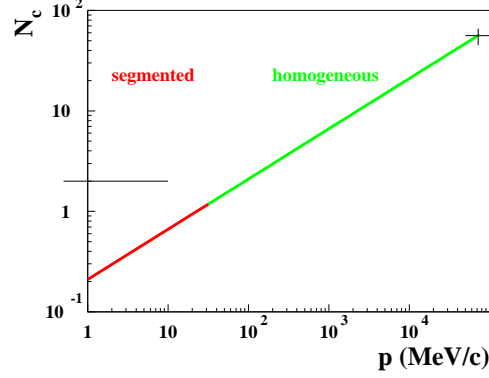


Fig. 4. Number of wafers that enable an optimum measurement, as a function of track momentum, obtained assuming a homogeneous-detector approximation (valid for the green part of the line).

by non-Gaussian noise contributions, such as that from Bremsstrahlung radiation.

Assuming that the single-track angular resolution for the two leptons translates to a single photon angular resolution with the same expression (See Fig. 1 of Bernard 2013b), I obtain a global description of the angular resolution of a segmented active target telescope, Figure 5. Significant contributions are

- the missing recoil at low energy;
- tracking and multiple scattering in the detector at high energy;
- multiple scattering in the conversion wafer, over the whole range.

We note the agreement with the results of simulations by e-ASTROGAM (De Angelis et al. 2018) even though they most likely used a pre-10.5 Geant4 release, that is, a recoil momentum distribution different from that of the Bethe-Heitler differential cross section (Gros & Bernard 2017b).

3. Polarization

The polarimetry of high-energy photons, that is, in the energy range for which the conversion of a photon can be recorded individually, is performed by the analysis of the distribution of the azimuthal angle, ϕ :

$$\frac{d\sigma}{d\phi} \propto (1 + A \times P \cos(2(\phi - \phi_0))), \quad (2)$$

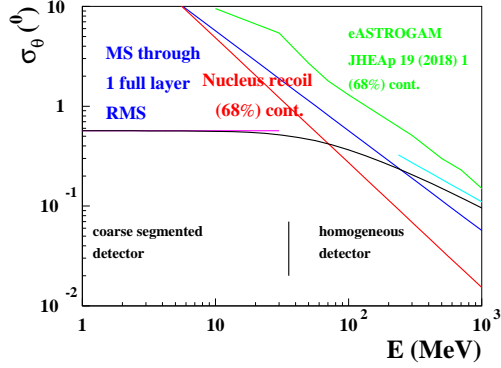


Fig. 5. Various contributions to the single photon angular resolution as a function of photon energy E .

where P is the linear polarization fraction of the incoming radiation, and A is the polarization asymmetry of the conversion process. The azimuthal angle of the event measures the orientation of the final state in the plane perpendicular to the direction of propagation of the incoming photon.

Polarimetry in the pair-conversion regime with silicon detectors has never been demonstrated, most likely due to a number of reasons, in particular the multiple scattering undergone by the two leptons during the propagation inside the detector (Fig. 6) and the difficulty of reconstructing the tracks close to the vertex with finite strip-width detectors.

The dilution of the polarization asymmetry due to multiple scattering in the conversion wafer, that is, of the effective value normalized to the QED value, $D = A_{\text{eff}}/A_{\text{QED}}$, can be computed simply by a convolution of the differential cross section eq. (2) with a resolution function, yielding $D = e^{-2\sigma_\phi^2}$, where σ_ϕ is the resolution of the measurement of ϕ . The calculation by (Kotov 1988) used the most probable value $\hat{\theta}_{+-} = E_0/E$, with $E_0 = 1.6$ MeV (Olsen 1963) of the pair opening angle θ_{+-} , to obtain $\sigma_\phi \approx (\theta_{0,e^+} \oplus \theta_{0,e^-})/\hat{\theta}_{+-} \approx 24 \text{ rad} \sqrt{e/X_0}$. A degradation of D by a factor of two is undergone for $\sigma_\phi = \sqrt{\ln 2}/2 \approx 0.59$ rad, that is, after a path length of $e \approx 10^{-3}X_0$, ($e \approx 100 \mu\text{m}$ for silicon or $e \approx 4 \mu\text{m}$ for tungsten).

The θ_{+-} distribution actually shows a tail at high values (Fig. 7 of Bernard 2018a) and

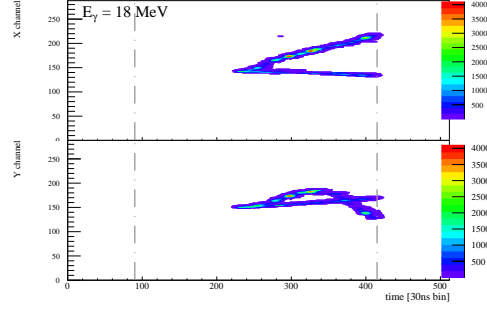


Fig. 6. Example of a conversion event for which the loss of azimuthal information during the propagation of the track in the detector is visible: (x, t) and (y, t) views of a 18 MeV γ -ray from the BL01 beam line at NewSUBARU (LASTI, Hyōgo U., Japan) converting to e^+e^- in the 2.1 bar Ar:Isobutane 95:5 gas of the HARPO TPC prototype. For this event, track crossing is seen to take place after $e \approx 10$ cm with $X_0 \approx 5600$ cm, that is, for $t \equiv e/X_0 \approx 1.8 \cdot 10^{-3}$.

there was hope that these events would be less affected by multiple scattering. Using the exact Bethe-Heitler event generator, I observed (Bernard 2013a) that the dilution is found to be larger (i.e. better) at large wafer thicknesses

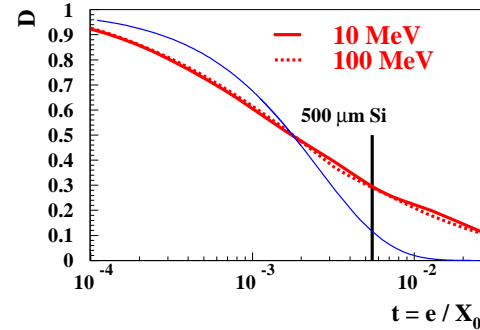


Fig. 7. Dilution of the polarization asymmetry, that is, the effective value normalized to the QED value, as a function of the wafer thickness traversed by the two leptons, normalized to the material radiation length (updated from Bernard 2013a, with the optimal definition of the azimuthal angle, which we found to be the azimuthal angle of the bisectrix of the azimuthal angles of the e^- and of the e^+ Gros & Bernard 2017a). The thin blue line is Kotov's E -independent, $\hat{\theta}_{+-}$ -based approximation. The thick red lines are from the full (5D) simulation.

(hundreds of microns) than that predicted assuming Kotov's approximation (Fig. 7).

4. Conclusions, recommendations

For most of their energy range, the all-silicon detector telescopes such as e-ASTROGAM and AMEGO that are being developed are thick detectors:

- the tracking-with-multiple-scattering contribution to the resolution angle is described by the analytical expressions of Section 2.1.1 of Frosini & Bernard (2017);
- the optimal number of wafers on which the Kalman-filter is applied is small and depends on photon energy; fitting longer track segments would make the result uselessly prone to bias induced by non Gaussian noise from radiation;
- the angular resolution should not depend on the depth of the conversion point in the detector.

At high energies,

- the homogeneous detector approximation is valid, and the use of a Kalman-filter-based tracking software is optimal.

At low energies,

- the measurement of the direction of the incoming photon can be performed simply from the positions measured in the two first wafers.
- the impossibility to measure the momentum of the recoiling nucleus is an important contribution to the angular resolution, making it mandatory to use an exact simulation of the distribution, in angle and in magnitude of the recoil, that is available in Geant4 release ≥ 10.5 .

Over most of the energy range, the containment angle induced by the unmeasured recoil momentum is universal, that is, it does not depend on the nature of the converter; only at the highest energies does the difference in the screening of the field of the atomic electrons induce a difference in the containment angle.

The transition between the low- and the high-energy regimes takes place in the $1.3 <$

$x < 2$ range, that is in, the $35 < p < 80 \text{ MeV}/c$ track momentum range for e-ASTROGAM. The contribution of the multiple scattering in the conversion wafer is important over the whole energy range, except for conversions in the very bottom part of the wafer. An event-dependent angular resolution could be considered, should the depth of the conversion point in the wafer be estimated from the deposited energy.

The study of the polarimetric performances of a detector necessitates the use of an exact event generator, and of an appropriate definition of the event azimuthal angle. The dilution of the polarization asymmetry due to multiple scattering in the conversion wafer is found to be much better, that is much higher, than that calculated in the most-probable opening angle approximation. The dilution is also found to be independent of the photon energy.

References

- Bernard, D. 2013a, Nucl. Instr. Meth. in Phys. Res. A, 729, 765
- Bernard, D. 2013b, Nucl. Instr. Meth. in Phys. Res. A, 701, 225
- Bernard, D. 2018a, Nucl. Instr. Meth. in Phys. Res. A, 899, 85
- Bernard, D. 2018b, Nucl. Instr. Meth. in Phys. Res. A, 936, 405
- De Angelis, A., et al. 2018, JHEAp, 19, 1
- Frosini, M. & Bernard, D. 2017, Nucl. Instr. Meth. A, 867, 182
- Gros, P., et al. 2018, Astropart. Phys., 97, 10
- Gros, P. & Bernard, D. 2017a, Astropart. Phys., 88, 30
- Gros, P. & Bernard, D. 2017b, Astropart. Phys., 88, 60
- Innes, W. R. 1993, Nucl. Instr. Meth. in Phys. Res. A, 329 238.
- Kotov, Iu. D. 1988, Space Sci. Rev., 49, 185
- Moiseev, A., et al. 2018, in 35th International Cosmic Ray Conference, PoS, 301, 798
- Olsen, H. 1963, Phys. Rev., 131, 406
- Ozaki, K., et al. 2016, Nucl. Instr. Meth. A, 833, 165
- Schönfelder, V. 2004, New Astron. Rev., 48, 193
- Takahashi, S., et al. 2015, Progress Theoret. Exper. Phys., 4, 043H01
- Tanabashi, M., et al. 2018, Phys. Rev. D, 98, 030001